



Study on the effects of hydraulically interconnected suspension system parameters on vehicle vibration characteristics

Arash Darvish Damavandi¹, Behrooz Mashadi², Masoud Masih-Tehrani^{*3}

Ph.D Student, School of automotive engineering, Iran University of Science and Technology, Tehran, Iran

Professor, School of automotive engineering, Iran University of Science and Technology, Tehran, Iran

Assistant Professor, School of automotive engineering, Iran University of Science and Technology, Tehran, Iran

ARTICLE INFO

Article history:

Received : 15 Apr 2023

Accepted: 1 Jul 2023

Published: 1 Aug 2023

Keywords:

Hydraulically Interconnected Suspension

Full vehicle model

Sensitivity analysis

Default HIS

Frequency and damping of system

ABSTRACT

This paper investigates the performance of the hydraulically interconnected suspension system with the full vehicle model of ride and handling. A sensitivity analysis has been performed by changing the coefficients of the cylinder and accumulator valves and the initial conditions of the accumulators in the default hydraulic circuits to determine the effect on the frequency and damping of the system response such as roll, pitch, and bounce. This study highlights the importance of the influence of all system parameters to investigate vehicle vibration characteristics. The results provide valuable insights for designers and engineers working on improving automotive suspension system performance. Damping and frequency of modes change up to 179% with the change of cylinder valves and 141% with the change of accumulator valves and 74% for the initial pressure of accumulators change in mentioned range.

Introduction

Physical laws and mathematical relationships can be used to model all natural phenomena [1], allowing for simulation of various systems using available software. However, many differential equations derived from mechanical and natural phenomena, such as hydraulic interconnected suspension systems, are non-linear. While solving non-linear differential equations is easy with current software, it is necessary to linearize the equations for simpler calculations and further analysis, including taking the equations into the state space. Simulation can aid in understanding the characteristics of different systems [2], including the interconnected suspension system discussed in this treatise.

Shao and colleagues [3] used a motion-mode energy method to select the dominant vehicle body mode as a control objective in real-time, resulting in improved responses for roll, pitch, and bounce. Lam et al. [4] controlled the roll angle in a sport utility vehicle with a fuzzy controller and pressure control unit. Xu et al. [5] studied the handling and ride specification of an SUV with a his and antiroll

bar, taking into consideration roll angle, tire forces, and the working space of struts.

Zhu et al. [6] improved roll response through accumulator pressure control in a model for roll-plane active his. Shao [7] studied anti-roll and anti-pitch configurations through modal analysis, demonstrating that roll and pitch stiffness were improved. Xu and Zhang [8] improved roll and pitch stiffness without affecting other modes by using modal analysis and combining roll and pitch his. Zhu et al. [9] used fuzzy, fuzzy PID and LQR controllers to improve roll angle response, concluding that the fuzzy PID controller was more stable and effective.

Hong et al. [10] improved bus handling by using a motion-mode energy method that considered roll response and mode energy. Xu et al. [11] showed that a roll and pitch independently tuned interconnected suspension (RPITIS) outperformed an anti-roll bar, improving longitudinal stability through tire forces, lateral stability through roll angle and yaw rate, and rollover critical factor of an SUV vehicle.

Yao et al. [12] mitigated the roll and pitch angle by using a dual-mode interconnected suspension,

* Corresponding Author

Email: masih@iust.ac.ir

<http://doi.org/10.22068/ase.2023.643>

with mode changing depending on the vehicle working condition and optimized mode switching threshold. Ding et al. [13] investigated the characteristics of the pitch-resistant his system, demonstrating that both top and bottom direction damper valves (DDVs) affected the vehicle body's pitch motion, and pitch damper valves (PDVs) were able to change the load distribution among wheel stations.

Wang et al. [14] used a hydraulically interconnected inerter-spring-damper suspension (HIISDS) to compensate for traditional passive suspension limitations and enhance ride and handling with a fuzzy control switching based on steering input. Zhu et al. [15] studied the road holding ability of his system with a comparison to an anti-roll bar through modal analysis. Saglam and Unlusoy [16] studied the roll and pitch angle response of a three-axle vehicle and showed that an improved hydro-pneumatic suspension system improved handling while only slightly degrading ride comfort due to increasing roll and pitch accelerations.

Tkachev and Zhang [17] showed an increased roll cancellation ability of an active his system for preventing rollover by using a half-car model. Zhang et al. [18] tuned the pitch and bounce response of a mini-vehicle through modal analysis and showed that cooperative control of bounce and pitch motion modes improved ride and handling.

Li et al. [19] improved the handling performance of an articulated six-axle vehicle through a proposed HIS system. Qi et al. [20] improved the ride and handling of a bus by using an electronic controller and air spring actuator to optimize tire forces and bounce acceleration, as well as lateral acceleration, roll angle, yaw rate, and rollover critical factor simultaneously. Wu et al. [21] optimized the anti-roll control parameter and point of switching in a dual-frequency-range semiactive suspension system to enhance the ride and anti-roll specification of a vehicle.

The main contribution of this paper is mentioned as follows:

1. Obtaining full vehicle model and mix it with HIS model
2. Investigating the impact of accumulator and cylinder valve change on frequency and damping of system modes such as roll and pitch and bounce
3. Investigating the effect of the accumulator's initial situation change on the system response
4. System response of roll, pitch, and bounce monitor with the change of initial pressure of accumulator and cylinder and accumulator valves

In this paper, in the first section, the full vehicle model of Ride and Handling was used to model the hydraulic interconnected suspension system, which is set up in MATLAB Simulink, and in the second section all the mentioned suspension parameters change in the specified range to investigate frequency and damping of roll, pitch, and bounce. By analyzing the system's responses with different inputs, the effect of changing each valve on the vehicle's dynamics were identified, and control rules will be extractable to improve its performance in various maneuvers. Figure 1 shows an overview of this study.

1. Methodology

2.1. Vehicle model

The full vehicle model incorporates the engine input torque, brake input torque, and steering input, which are dependent on the vehicle's driver input, allowing for simulation of various maneuvers. The model is composed of three sub-systems: ride, handling, and tires, each with its own input and output. The ride system's input is the longitudinal, lateral acceleration and rate of yaw angle, producing the vertical force of the tires and roll angle as output.

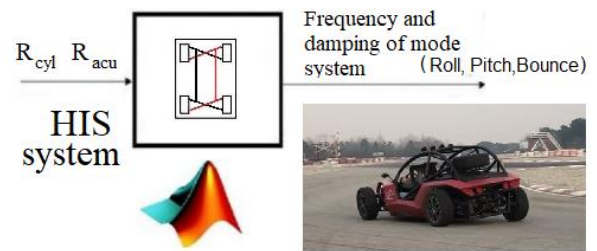


Figure 1: overview of this study

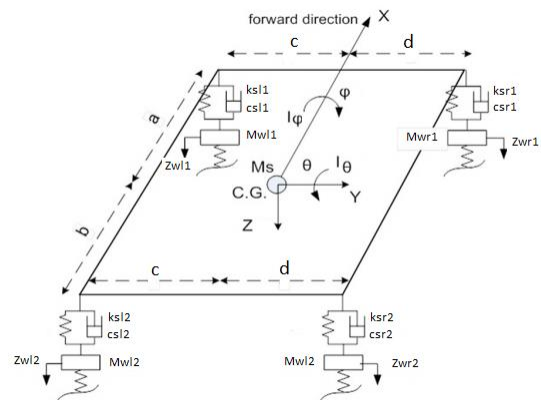


Figure 2: General overview of ride model

The tire subsystem's input is the slip angles and vertical force of the tires, generating the lateral and longitudinal force of the tires and self-aligning moment of tires as output. These outputs, along with the engine input torque, brake input torque, and steering input, serve as inputs for the handling system while yaw rate and lateral and longitudinal acceleration of the vehicle and slip angles of tires are as output of this subsystem. Figure 3 illustrates the information flow within the full vehicle model model.

At first, seven degrees of freedom of the ride subsystem are considered, which are available in Equations (1) to (7). The degrees of freedom are roll, pitch, and bounce, and four vertical displacements of the wheels. The input of the system is the longitudinal, lateral accelerations and yaw rate and the output is the

vertical force of the tires plus roll degree. Parameters in Equations (1) to (10) are shown in Figure 2. Also, F_s, F_d, F_t are a force in spring and damper and tires respectively.

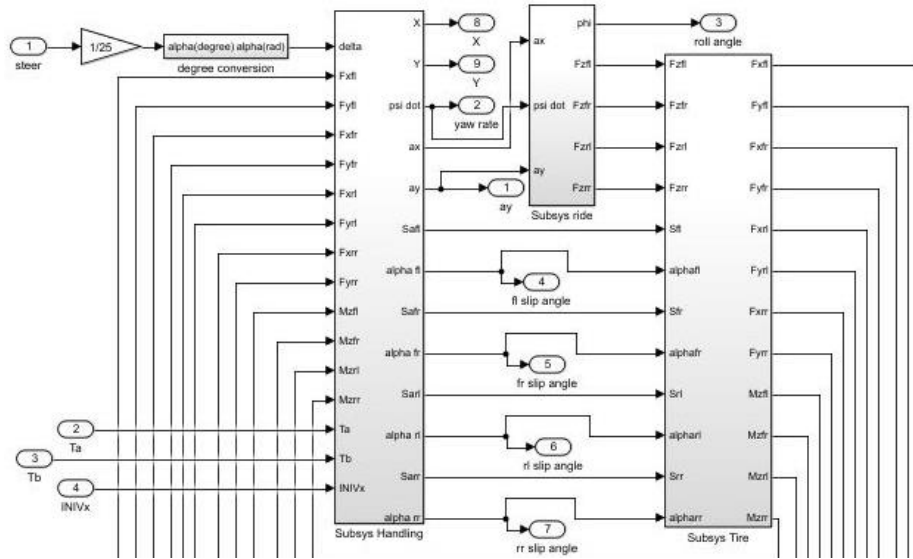


Figure 3: General scheme of information flow in the full vehicle model

$$m_s \ddot{Z} = F_{sl1} + F_{dl1} + F_{sr1} + F_{dr1} + F_{sl2} + F_{dl2} + F_{sr2} + F_{dr2} \quad (1)$$

$$I_\phi \ddot{\phi} = (F_{sl1} + F_{dl1} + F_{sl2} + F_{dl2})c - (F_{sr1} + F_{dr1} + F_{sr2} + F_{dr2})d \quad (2)$$

$$I_\theta \ddot{\theta} = (F_{sl2} + F_{dl2} + F_{sr2} + F_{dr2})b - (F_{sr1} + F_{dr1} + F_{sr2} + F_{dr2})a \quad (3)$$

$$m_{wl1} \ddot{Z}_{wl1} = F_{tl1} - F_{sl1} - F_{dl1} \quad (4)$$

$$m_{wr1} \ddot{Z}_{wr1} = F_{tr1} - F_{sr1} - F_{dr1} \quad (5)$$

$$m_{wl2} \ddot{Z}_{wl2} = F_{tl2} - F_{sl2} - F_{dl2} \quad (6)$$

$$m_{wr2} \ddot{Z}_{wr2} = F_{tr2} - F_{sr2} - F_{dr2} \quad (7)$$

that the vertical force of the tires is obtained from Equation (8).

$$F_t = K_t(z_0 - z_w) \quad (8)$$

It should be noted that, equations (1) to (7) are just for the ride model without any lateral and longitudinal acceleration; if longitudinal and lateral accelerations are entered into the model, equations (2) and (3) will change to Equations (9) and (10). In result, equations (9) and (10) are complete form of equations (2) and (3) and will be used in 14 DOF model.

$$I_\theta \ddot{\theta} = m_s a_x (\Delta h) + m_s g (\Delta h) \theta + (F_{sl2} + F_{dl2} + F_{sr2} + F_{dr2})b - (F_{sr1} + F_{dr1} + F_{sl1} + F_{dl1})a \quad (9)$$

$$(I_\phi + m_s (\Delta h)^2) \ddot{\phi} = m_s a_y (\Delta h) \cos \phi - m_s g (\Delta h) \sin \phi + (F_{sl1} + F_{dl1} + F_{sl2} + F_{dl2})c - (F_{sr1} + F_{dr1} + F_{sr2} + F_{dr2})d \quad (10)$$

The inputs of the vertical force of the tires are applied into the subsystem of the tires along with the slip angles which are the output of the handling subsystem. It determines the longitudinal and lateral forces and torque in each wheel. A simple magic formula is used in this subsystem. This subsystem has four degrees of freedom of wheel rotation. The output of this system enters the

handling subsystem. This subsystem has three degrees of freedom. The longitudinal and lateral displacement of the center of mass and the yaw angle are available in Equations (11) to (15).

$$a_x = \dot{v}_x - v_y \dot{\gamma} \quad (11)$$

$$m_s a_x = F_{xl1} \cos \delta - F_{yl1} \sin \delta + F_{xr1} \cos \delta - F_{yr1} \sin \delta + F_{xl2} + F_{xr2} \quad (12)$$

$$a_y = \dot{v}_y + v_x \dot{\gamma} \quad (13)$$

$$m_s a_y = F_{yl1} \cos \delta + F_{xl1} \sin \delta + F_{yr1} \cos \delta + F_{xr1} \sin \delta + F_{yl2} + F_{yr2} \quad (14)$$

$$I_y \ddot{\gamma} = +cF_{xl1} \cos \delta - cF_{xr1} \cos \delta + cF_{xl2} - cF_{xr2} - cF_{yl1} \sin \delta + cF_{yr1} \sin \delta + aF_{xl1} \sin \delta + aF_{yl1} \cos \delta + aF_{xr1} \sin \delta + aF_{yr1} \cos \delta - bF_{yl2} - bF_{yr2} + M_{zl1} + M_{zr1} + M_{zl2} + M_{zr2} \quad (15)$$

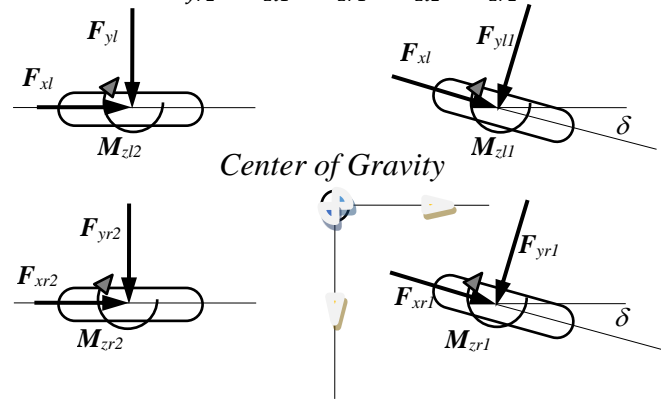


Figure 4: General scheme of the symbols used in the handling model

[DOI: 10.22068/ase.2023.643] [Downloaded from ce.iust.ac.ir on 2026-06-07]

where M in Figure 4 and Equation (15) is the torque of the wheels and the speed of the tires is obtained from the Equations (16) to (19). And of course, its output can be used to calculate wheel slip angles and longitudinal and lateral accelerations of the center of mass. Figure 4 depicts the general outline of the symbols used in the handling model.

$$I_w \dot{\omega}_{l1} = T_{dl1} - T_{bl1} - F_{xl1} R_w \quad (16)$$

$$I_w \dot{\omega}_{r1} = T_{dr1} - T_{br1} - F_{xr1} R_w \quad (17)$$

$$I_w \dot{\omega}_{l2} = T_{dl2} - T_{bl2} - F_{xl2} R_w \quad (18)$$

$$I_w \dot{\omega}_{r2} = T_{dr2} - T_{br2} - F_{xr2} R_w \quad (19)$$

2.2. HIS model

The overall outline of the ride subsystem is as follows. As it is clear below, you can add the force input to the four wheels. Below is the hydraulically connected subsystem, which changes in the length of the struts is its input and its output is forces. This force applies the sprung and unsprung mass in opposite ways. The Equations of the HIS subsystem are given in Equations (20) to (49) above.

In the next step, the equations of forces added to the system equipped with HIS are extracted. The general equation of the system is in Equations (20) to (22), where the matrix A and P are the cross-sectional areas and pressures of each of the double-acting cylinders, respectively.

Figure 5 shows an overview of the HIS subsystem. HIS parameters which are used in this section have shown in Figure 5.

$$M\ddot{Z} + C\dot{Z} + KZ + D_1AP(t) = F_{ext}(t) \quad (20)$$

$$A = \text{diag}([A_T^1 A_B^1 A_T^2 A_B^2 A_T^3 A_B^3 A_T^4 A_B^4]) \quad (21)$$

$$P = [P_T^1 P_B^1 P_T^2 P_B^2 P_T^3 P_B^3 P_T^4 P_B^4] \quad (22)$$

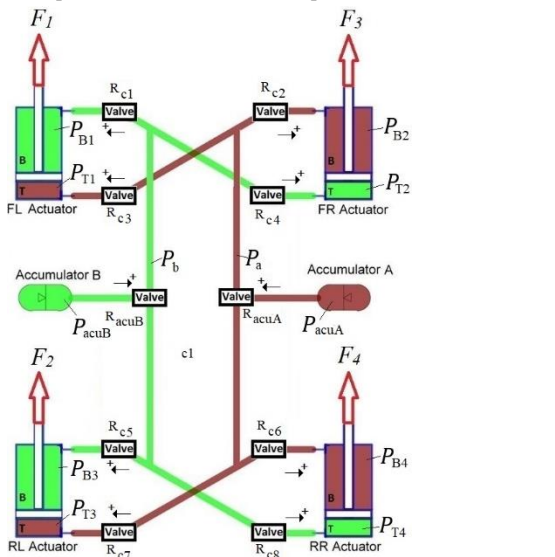


Figure 5: General overview of HIS subsystem

Therefore, the forces that apply from the cylinders on both sides are given in Equations (23) to (26).

$$F_1 = A_{T1}P_a - A_{B1}P_b \quad (23)$$

$$F_2 = A_{T2}P_b - A_{B2}P_a \quad (24)$$

$$F_3 = A_{T3}P_a - A_{B3}P_b \quad (25)$$

$$F_4 = A_{T4}P_b - A_{B4}P_a \quad (26)$$

And the vehicle Equations which were generally given in equations (1) to (7), the double-acting cylinder force terms are added in the form of equations (27) to (29) which are given below.

$$F_1 + F_2 + F_3 + F_4 = P_A(2(A_T - A_B)) + P_B(2(A_T - A_B)) \quad (27)$$

$$-aF_1 - aF_2 + bF_3 + bF_4 = P_A(b - a)(A_T - A_B) + P_B(b - a)(A_T - A_B) \quad (28)$$

$$-dF_1 + cF_2 - dF_3 + cF_4 = P_A(-2dA_T - 2cA_B) + P_B(2cA_T + 2dA_B) \quad (29)$$

And the accumulator is modeled through Equation (30), which is obtained from the derivation of the adiabatic gas model.

$$\dot{P}_a = \frac{\gamma Q_a P_a}{V_p} \left(\frac{P_a}{P_p}\right)^{\frac{1}{\gamma}} \quad (30)$$

And the pressures of each of the separate circuits are obtained from equations (31) to (38), where Q is the output flow rate from each of the cylinders or the input to the accumulators and R is the coefficient of valves. It should be noted that the following system is related to the default HIS model.

$$P_T^1 = P_a + R_{c1}Q_T^1 \quad (31)$$

$$P_B^2 = P_a + R_{c4}Q_B^2 \quad (32)$$

$$P_T^3 = P_a + R_{c7}Q_T^3 \quad (33)$$

$$P_B^4 = P_a + R_{c6}Q_B^4 \quad (34)$$

$$P_B^1 = P_b + R_{c2}Q_B^1 \quad (35)$$

$$P_T^2 = P_b + R_{c3}Q_T^2 \quad (36)$$

$$P_B^3 = P_b + R_{c8}Q_B^3 \quad (37)$$

$$P_T^4 = P_b + R_{c5}Q_T^4 \quad (38)$$

And the input flow rate in accumulators A and B is obtained from equations (39) and (40).

$$Q_A = Q_T^1 + Q_B^2 + Q_T^3 + Q_B^4 \quad (39)$$

$$Q_B = Q_B^1 + Q_T^2 + Q_B^3 + Q_T^4 \quad (40)$$

According to Equation (30), the equation of the pressure change rate of two accumulators is calculated as equations (41) and (42).

$$\begin{aligned} \dot{P}_A &= \eta_A Q_{acuA} = \eta_A(Q_T^1 + Q_B^2 + Q_T^3 + Q_B^4) \quad (41) \\ &= \eta_A(\dot{Z}(2(A_T - A_B)) + \dot{\theta}((b - a)(A_T - A_B)) + \dot{\varphi}(-2dA_T - 2cA_B) + \dot{z}_{mr1}(A_B) + \dot{z}_{mr1}(-A_T) + \dot{z}_{mr2}(A_B) + \dot{z}_{mr2}(-A_T)) \end{aligned}$$

$$\begin{aligned} \dot{P}_B &= \eta_B Q_{acuB} = \eta_B(Q_B^1 + Q_T^2 + Q_B^3 + Q_T^4) \quad (42) \\ &= \eta_B(\dot{Z}(2(A_T - A_B)) + \dot{\theta}((b - a)(A_T - A_B)) + \dot{\varphi}(2dA_T + 2cA_B) + \dot{z}_{mr1}(-A_T) + \dot{z}_{mr1}(A_B) + \dot{z}_{mr2}(-A_T) + \dot{z}_{mr2}(A_B)) \end{aligned}$$

where η_A and η_B are calculated from Equation (43) respectively.

$$\eta_A = \frac{\gamma P_{mean-acuA}}{V_{prA}} \left(\frac{\gamma P_{mean-acuA}}{P_{prA}}\right)^{\frac{1}{\gamma}} \quad (43)$$

$$\eta_B = \frac{\gamma P_{mean-acuB}}{V_{prB}} \left(\frac{\gamma P_{mean-acuB}}{P_{prB}}\right)^{\frac{1}{\gamma}}$$

In examining the initial conditions of the problem, it should be considered that after installing the hydraulically interconnected suspension system to the vehicle, the height of the center of mass of the car changes, and the roll angle of the car also changes. It is important to note that in all the circuits, the pitch angle of the vehicle in the static state is equal to zero. The equations (44) to (49) are related to the calculation of the static state.

$$2(F_1 + F_3) = (k_{sr1} + k_{sl1} + k_{sr2} + k_{sl2})Z_{ES-HIS} + (-k_{sr1}a - k_{sl1}a + k_{sr2}b + k_{sl2}b)\theta_{ES-HIS} + Mg \quad (44)$$

$$-2aF_1 + 2bF_3 = (-k_{sr1}a - k_{sl1}a + k_{sr2}b + k_{sl2}b)Z_{ES-HIS} + (k_{sr1}a^2 + k_{sl1}a^2 + k_{sr2}b^2 + k_{sl2}b^2)\theta_{ES-HIS} \quad (45)$$

$$F_1 = A_T P_A - A_B P_B \quad (46)$$

$$F_3 = A_T P_A - A_B P_B \quad (47)$$

$$P_A = \frac{P_{praA} V_{praA}^\gamma}{(V_{praA} - \left(\frac{(A_T - A_B)(Z_{ES-HIS} - a\theta_{ES-HIS})}{(A_T - A_B)(Z_{ES-HIS} + b\theta_{ES-HIS})} \right)^\gamma)} \quad (48)$$

$$P_B = \frac{P_{praB} V_{praB}^\gamma}{(V_{praB} - \left(\frac{(A_T - A_B)(Z_{ES-HIS} - a\theta_{ES-HIS})}{(A_T - A_B)(Z_{ES-HIS} + b\theta_{ES-HIS})} \right)^\gamma)} \quad (49)$$

In the following, verifying the responses of the full vehicle model is done in previous research by the same researcher [22].

It should be noted that the frequency of the system is obtained from the distance between the two peaks of the response and damping from the logarithmic reduction method from Equation (51) [23].

$$\delta = \frac{1}{n} \ln \left| \frac{x_1}{x_{n+1}} \right| \quad (50)$$

$$Damping = \zeta = \frac{\delta}{\sqrt{4\pi^2 + \delta^2}} \quad (51)$$

2.3. Parameter study

As mentioned before, the parameters of the system that have been examined with changes are two valves of accumulators and eight valves of the cylinder, and the initial pressure of the accumulators. These parameters are respectively introduced in the text to $R_{acuA} - R_{acuB}$ and $R_{c1} - R_{c8}$ and P_0 .

The change range of each parameter is specified below and these ranges are extractable from previous studies.

$$60\% < R_{acuA} - R_{acuB} < 100\%$$

$$60\% < R_{c1} - R_{c8} < 100\%$$

$$50 \text{ kPa} < P_0 < 500 \text{ kPa}$$

3. Result and discussion

To analyze and understand the system, the idea of superposition is used, in the sense that the effect of different parameters is investigated in different states.

3.1. Analysing impact of accumulator valves on system response

At first, we keep the cylinder valves constant and observe the responses of the system by increasing the coefficient of the two accumulator valves in the same way (the valve becomes more closed).

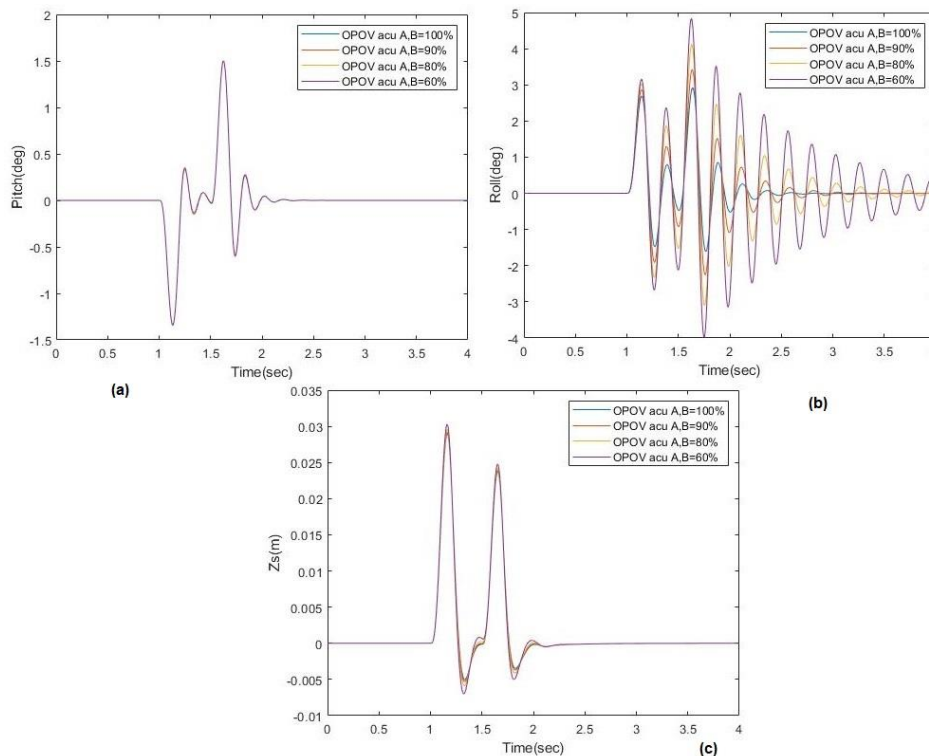


Figure 6: The response of (a) pitch angle (deg) (b) roll angle (deg) (c) bounce (m) in terms of time (sec) in the half-bump sine wave maneuver for different coefficients of the accumulator and constant valve coefficients

Effect of Hydraulically interconnected suspension system parameters on response of system

As can be seen in Figure 6(a), the symmetrical increase of the accumulator valves coefficient does not change the response of the pitch angle, while according to Figure 6(b), the symmetrical increase of the coefficient of the accumulator valves has a significant effect on the roll response and increases the roll angle. While according to Figure 6(c), the changes in the accumulator valves will not have much effect on the response of the bounce.

In the following, we keep the cylinder valves constant and observe the responses of the system by increasing the valve coefficient of accumulator A and keeping the valve coefficient of accumulator B constant. As can be seen in Figure 7(a), the asymmetric increase of the accumulator valves changes the response of the pitch angle only slightly, which is not significant; If according to

Figure 7(b), the asymmetric increase of the coefficient of the accumulator valves will have a significant effect on the roll response and will increase the roll angle. The noteworthy point is that the effect on the roll angle response, in this case, is less than the case of symmetrical change of the accumulator valves, so it is considered that the two valves are parallel to each other and increasing the coefficient of each one has a greater effect on the response of the roll angle of the system. And while it can be seen in Figure 7(c) that the asymmetric changes of the accumulator valves had a greater effect on the response of bounce compared to the case of symmetrical changes. of course, it is necessary to mention that the asymmetric increase of the coefficient of the accumulator did not have a positive effect on the response of the bounce.

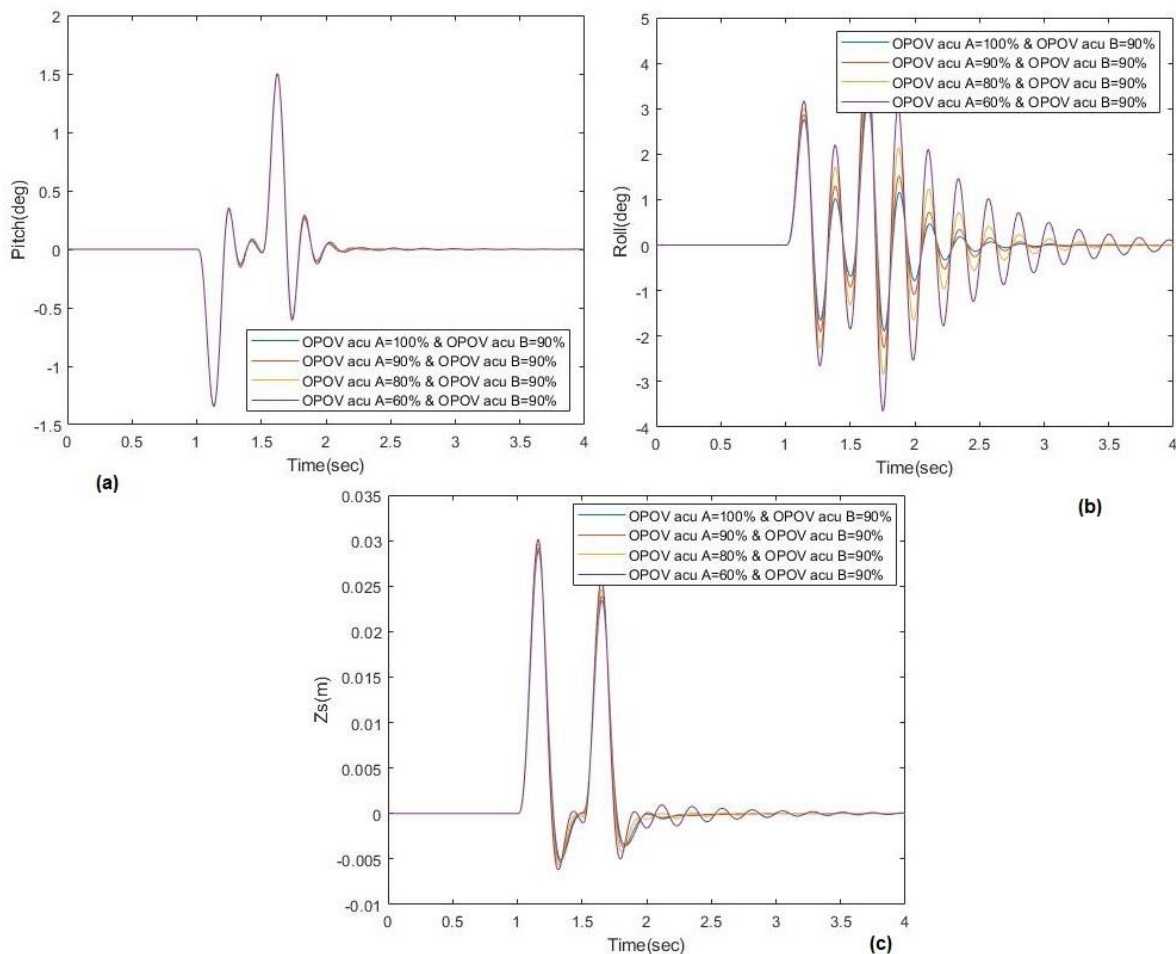


Figure 7: The response of (a) pitch angle (deg) (b) roll angle (deg) (c) bounce (m) in terms of time (sec) in the half-bump maneuver for different coefficients of accumulator valve A and constant valve coefficients

In changing the coefficients of accumulator valve B and keeping accumulator valve A constant, there is no additional analysis except that the responses are the same if the coefficients of the accumulator replace. The car's maneuver involves a left front wheel step input, and Table 1 shows the damping and frequency of different modes (roll, pitch, and bounce) in the system under varying coefficient levels of accumulator valves when cylinder valves are closed. Table 1 shows that damping

decreases and frequency increases at a specified rate when the accumulator valves area tightens respectively. No significant changes are observed in pitch and bounce modes. It shows that accumulator valves play a significant role in roll mode and an unimportant role in pitch and bounce mode. there is a 75% and 13% change in frequency and damping of roll respectively. OPOV, acu A, Con system, and Peak in Table 1 stand for the “opening percentage of valve”, the accumulator A, the

conventional suspension system without HIS, and the maximum response, respectively. It should be noted that the Freq. and damping in Table 1 are obtained from Equation (51).

Table 1: Damping and frequency of different modes of the system in different coefficient of accumulator valves with closed cylinder valves

		Roll		
OPOV acu B	OPOV acu A	Freq. (Hz)	Peak (deg)	Damping
100	100	3.73(-)	2.6(-)	0.27(-)
90	90	4.03(8%)	2.7(6%)	0.14(-48%)
80	80	4.15(11%)	2.9(12%)	0.10(-61%)
60	60	4.23(13%)	3.1(20%)	0.07(-75%)
Con system		1.40(-62%)	2.4(-5%)	0.20(-27%)
		Pitch		
OPOV acu B	OPOV acu A	Freq. (Hz)	Peak (deg)	Damping
100	100	5.52(-)	-1.42(-)	0.11(-)
90	90	5.52(0%)	-1.42(0%)	0.11(0%)
80	80	5.52(0%)	-1.42(0%)	0.11(0%)
60	60	5.55(0,05%)	-1.42(0%)	0.11(0,8%)
Con system		0.97(-82%)	-1.38(-3%)	0.28(141%)
		Bounce		
OPOV acu B	OPOV acu A	Freq. (Hz)	Peak (m)	Damping
100	100	5.29(-)	0.034(-)	1(-)
90	90	5.35(1%)	0.034(0%)	1(0%)
80	80	5.38(1%)	0.033(-3%)	1(0%)
60	60	5.47(3%)	0.033(-3%)	1(0%)
Con system		1.11(78%)	0.034(0%)	0.17(-82%)

3.2. Analysing impact of cylinder valves on system response

In the following, we keep the valves of the accumulators constant and check the responses of the system by increasing the cylinder coefficient of eight-cylinder valves in the same way. As can be seen in Figure 8(a), the symmetrical increase of the cylinder valves increases the response of the pitch angle, and as can be seen in Figure 8(b), the symmetrical increase of the coefficient of the cylinder valves also has a significant effect on roll response and will also increase the roll angle. And as shown in Figure 8(c), the changes in the cylinder valves will also have a great impact on the response of the bounce. of course, these answers were completely predictable because raising the coefficients of the accumulator valves is exactly like raising the coefficients of the struts and makes the system hard, and in maneuvers such as half a sine bump where the stimulation is from the roadside, the response moves towards becoming undesirable. But this issue brings to mind the idea that it is better to increase or decrease the necessary valve coefficients. In our problem, it may be necessary to change the coefficients of the cylinder valve that is on the bump.

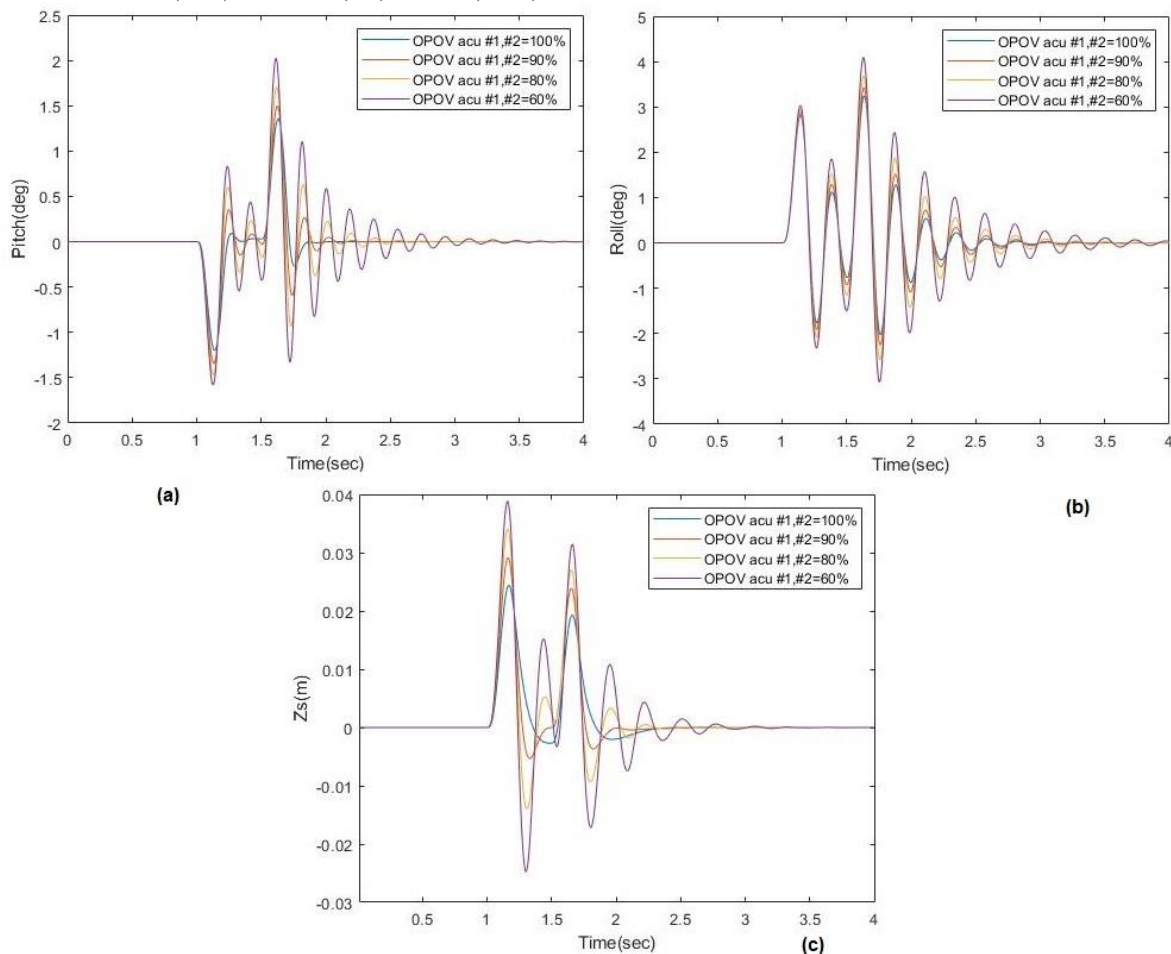


Figure 8: The response of (a) pitch angle (deg) (b) roll angle (deg) (c) bounce (m) in terms of time (sec) in the half-bump maneuver for constant coefficients of accumulator valves and different valve coefficients

Therefore, in the following, we keep the valves of the accumulators constant and also the coefficients of the cylinder valves, except for the coefficients of the valve located on the bump, and check the responses of the system. As is predictable, all the mentioned responses have improved when we open the mentioned cylinder valves. It is worth mentioning that in this maneuver the front left wheel is engaged first and after some time the rear left wheel is involved in this maneuver, we only opened the valves of the front left cylinder while the correct thing was that after the first wheel passed, the valves of The front left cylinder was closed and the valves of the rear left cylinder were opened. Therefore, our answers are correct in the range of the first rise of the system.

In the end, it seems that if there is a force in the HIS cylinders in the direction of worsening the dynamic situation of the car; It should be weakened or vice versa. If the lower chamber pressure decreases; The upward force is reduced and the pressure drop in the upper chamber also weakens the downward force. Now, if the car is in a vibrating road maneuver; The force that contributes to the roll must be reduced. Now, if the problem is to improve the dynamic condition of the car in cornering, in order to reduce the yaw angle rate, the vertical force of the rear tires should be more than the front tires, because of that, the lateral force of the rear tire is greater than the front, and this causes a resistant torque to be applied around the yaw. And also if the lateral acceleration tilts the body of the car and the car rolls; The fluid flow moves toward the accumulator. Tightening the accumulator valve, also has a double pressure on the fluid, which causes the return of the roll. Of course, it is necessary to determine, for example, whether the roll angle created in the car is due to lateral acceleration or not; which in any case is considered logical for opening and closing or raising and lowering the coefficients of the cylinder and accumulator valves.

In the next step, the effect of accumulator valves and cylinder valves, as well as accumulator parameters such as initial pressure, on damping and frequency of different system modes such as roll, pitch, and bounce are investigated.

Table 2 shows the damping and frequency of different modes under various coefficient levels of cylinder valves while accumulator valves are closed. dissimilar previously, no significant changes are observed in roll mode, but there are substantial changes in pitch and bounce modes. As it can be seen in roll mode max change percentage is 3% which is ignorable. When it comes to pitch mode, in damping and frequency 130% and 28% change are observed respectively. And when bounce takes into consideration damping and frequency 179% and 42% change is observed

respectively. The #1 and #2 in Table 2 stand for the first and second double acting cylinders.

Table 2: Damping and frequency of different modes of the system in different coefficient of the mentioned cylinder valves with closed accumulator valves

Roll				
OPOV #2	OPOV #1	Freq. (Hz)	Peak (deg)	Damping
100	100	4.25(-)	2.81(-)	0.06(-)
90	90	4.27(0.4%)	2.91(3%)	0.07(3%)
80	80	4.25(0%)	2.99(6%)	0.07(3%)
60	60	4.23(-0.4%)	3.13(11%)	0.07(3%)
Pitch				
OPOV #2	OPOV #1	Freq. (Hz)	Peak (deg)	Damping
100	100	7.75(-)	-0.98(-)	0.05(-)
90	90	6.49(-16%)	-1.11(13%)	0.09(80%)
80	80	6.09(-21%)	-1.23(25%)	0.11(130%)
60	60	5.55(-28%)	-1.42(45%)	0.11(130%)
Bounce				
OPOV #2	OPOV #1	Freq. (Hz)	Peak (m)	Damping
100	100	9.52(-)	0.031(-)	0.34(-)
90	90	7.19(-24%)	0.031(0.9%)	0.71(109%)
80	80	5.55(-41%)	0.032(2%)	0.85(150%)
60	60	5.47(-42%)	0.034(8%)	0.95(179%)

3.3. Analysing impact of initial situation of accumulators on system response

Table 3 examines the impact of the initial accumulator pressure, revealing noticeable changes in roll mode damping and pitch mode frequency as pressure changes. The left front wheel step input is still applied, but now the cylinder and accumulator valves are completely open. When it comes to the initial pressure of accumulators, there is no important change in pitch and bounce mode but in roll mode, damping, and frequency 74% and 62% opportunity change respectively.

Table 3: Damping and frequency of different modes of the system at different levels of initial pressure of the accumulator with accumulator and cylinder valves opened

Roll			
P_0	Freq. (Hz)	Peak (deg)	Damping
$P_0 = 500 \text{ kPa}$	1.72(-)	2.73(-)	0.16(-)
$P_0 = 250 \text{ kPa}$	1.88(9%)	2.93(7%)	0.13(-19%)
$P_0 = 125 \text{ kPa}$	2.14(19%)	3.40(24%)	0.09(-39%)
$P_0 = 50 \text{ kPa}$	2.80(62%)	3.78(38%)	0.04(-74%)
Pitch			
P_0	Freq. (Hz)	Peak (deg)	Damping
$P_0 = 500 \text{ kPa}$	0.96(-)	-1.38(-)	0.27(-)
$P_0 = 250 \text{ kPa}$	0.96(0,5%)	-1.37(-0,1%)	0.27(-0,4%)
$P_0 = 125 \text{ kPa}$	0.97(1%)	-1.37(-0,1%)	0.25(-6%)
$P_0 = 50 \text{ kPa}$	0.97(1%)	-1.36(-0,2%)	0.23(-12%)
Bounce			
P_0	Freq. (Hz)	Peak (m)	Damping
$P_0 = 500 \text{ kPa}$	1.12(-)	0.039(-)	0.17(-)
$P_0 = 250 \text{ kPa}$	1.12(0,3%)	0.039(1%)	0.17(1%)
$P_0 = 125 \text{ kPa}$	1.13(0,8%)	0.041(5%)	0.17(1%)
$P_0 = 50 \text{ kPa}$	1.14(1,8%)	0.046(17%)	0.17(2%)

4. Conclusions

The simulation analyzed the impact of system parameters, such as accumulator valves, cylinder valves, and initial conditions of accumulators, on the system modes of roll, pitch, and bounce. The study also examined the effect of resource changes on the frequency and damping of each system mode. The results indicated that closing accumulator valves increased the roll response frequency while decreasing its damping. No significant change was observed in pitch and bounce mode. Additionally, the study investigated the damping and frequency of other modes under different cylinder valve coefficients while accumulator valves were closed. The impact of initial pressure on accumulators was also analyzed, revealing a noticeable change in the damping mode of the pitch. Overall, the simulation provided insights into how different system parameters affect suspension dynamics.

In conclusion, the development of hydraulically interconnected suspension has shown great potential for improving vehicle performance and safety. Although existing systems have demonstrated effective results, further research can focus on optimizing and advancing this technology in terms of ride comfort, handling, and energy efficiency. Some potential future work could involve exploring new materials and designs for the hydraulic lines and components, integrating electronic controls for more precise and adaptive suspension response, and investigating potential uses of machine learning and artificial intelligence to enhance system optimization and predictability. It is clear that the potential benefits of hydraulically interconnected suspension are substantial, and continued research and innovation will undoubtedly bring new and exciting improvements to this vital automotive technology.

To provide a brief overview of this study's achievements:

1. 75% and 13% change in frequency and damping of roll mode with accumulator valve coefficient change respectively.
2. In pitch mode, damping, and frequency have 130% and 28% changes. And bounce has damping and frequency changes of 179% and 42% change respectively with the change of cylinder valve coefficient change.
3. In roll mode with changing initial pressure of accumulator, damping and frequency opportunities 74% and 62% change respectively.

In future works, it is suggested that considering the effect of cylinder and accumulator valves on the system

responses, to develop control rules for better control of the system.

References

- [1] Najafi, A., & Masih-Tehrani, M. (2022). Roll stability enhancement in a full dynamic ground-tour vehicle model based on series active variable-geometry suspension. *International Journal of Vehicle Performance*, 8(2-3), 188-223.
- [2] Boluhari, S. M., Masih-Tehrani, M., Yahyaei, R., & Marzbanrad, J. (2020). Seat-driver vibration parameters effect on horizontal driver acceleration and its relationship to driver mass. *International Journal of Hydromechatronics*, 3(3), 281-296.
- [3] Shao X, Zhang N, Du H, et al. Fuzzy control of hydraulically interconnected suspension with configuration switching. In: *Proceedings of 2013 IEEE international conference on vehicular electronics and safety*, Dongguan, China, 28–30 July 2013, pp.66–71. IEEE.
- [4] Lam Q, Wang L and Zhang N. Experimental implementation of a fuzzy controller for an active hydraulically interconnected suspension on a sport utility vehicle. In: *2013 IEEE Intelligent Vehicles Symposium (IV)*, Gold Coast, QLD, Australia, 23–26 June 2013, pp.383–390. IEEE.
- [5] Xu G, Roser HM and Zhang N. Experimental study of a roll-plane hydraulically interconnected suspension system under vehicle articulation mode. In: *Proceedings of the ASME international mechanical engineering congress and exposition (IMECE)*, San Diego, California, 15–21 November 2013.
- [6] Zhu S, Du H, Zhang N, et al. Development of a new model for roll-plane active hydraulically interconnected suspension. *SAE Int J Passeng Cars Mech Syst* 2014; 7(2): 447–457.
- [7] Shao X. Modeling and model analysis of a full-car fitted with an anti-pitch anti-roll hydraulically interconnected suspension. *SAE technical paper* 2014-01-0849, 2014.
- [8] Xu G and Zhang N. Characteristic analysis of roll and pitch independently controlled hydraulically interconnected suspension. *SAE Int J Commer Veh* 2014; 7(1):170–176.
- [9] Zhu S, Du H and Zhang N. Development and implementation of fuzzy, fuzzy PID and LQR controllers for an roll-plane active Hydraulically Interconnected Suspension. In: *2014 IEEE international conference on fuzzy systems (FUZZ-IEEE)*, Beijing, China, 6–11 July 2014, pp.2017–2024. IEEE.
- [10] Hong H, Wang L, Zheng M, et al. Handling analysis of a vehicle fitted with roll-plane hydraulically interconnected suspension using motion-mode energy

Effect of Hydraulically interconnected suspension system parameters on response of system

method. *SAE Int J Passeng Cars Mech Syst* 2014; 7(1): 48–57.

[11] Xu G, Zhang N and Roser HM. Roll and pitch independently tuned interconnected suspension: modelling and dynamic analysis. *Veh Syst Dyn* 2015; 53(12): 1830–1849.

[12] Yao Q, Zhang X, Guo K, et al. Study on a novel dual-mode interconnected suspension. *Int J Veh Des* 2015; 68(1–3): 81–103.

[13] Ding F, Han X, Zhang N, et al. Characteristic analysis of pitch-resistant hydraulically interconnected suspensions for two-axle vehicles. *J Vib Control* 2015; 21(16): 3167–3188.

[14] Wang R, Ye Q, Sun Z, et al. A study of the hydraulically interconnected inerter-spring damper suspension system. *Mech Based Des Struct Mach* 2017; 45(4): 415–429.

[15] Zhu S, Xu G, Tkachev A, et al. Comparison of the road-holding abilities of a roll-plane hydraulically interconnected suspension system and an anti-roll bar system. *Proc IMechE, Part D: J Automobile Engineering* 2017; 231(11): 1540–1557.

[16] Saglam F and Unilusory YS. Modelling and simulation of a three-axle vehicle with interconnected hydro-pneumatic suspension system. In: *Proceedings of the 36th FISITA World Automotive Congress, Busan, South Korea, 26–30 September 2016*.

[17] Tkachev AA and Zhang N. Active hydraulically interconnected suspension. modeling and simulation. *SAE technical paper 2017-01-1561*, 2017.

[18] Zhang J, Deng Y, Zhang N, et al. Vibration performance analysis of a mining vehicle with bounce and pitch tuned hydraulically interconnected suspension. *Chin J Mech Eng* 2019; 32(1): 5.

[19] Li H, Li S and Sun W. Vibration and handling stability analysis of articulated vehicle with hydraulically interconnected suspension. *J Vib Control* 2019; 25(13): 1899–1913.

[20] Qi H, Chen Y, Zhang N, et al. Improvement of both handling stability and ride of a vehicle via coupled hydraulically interconnected suspension and electronic controlled air spring. *Proc IMechE, Part D: J Automobile Engineering* 2020; 234(2–3): 552–571.

[21] Wu X, Qiu X, Zhou B, et al. HIS-based semiactive suspension dual-frequency-range switching control to improve ride and antiroll performance. *Shock Vib* 2019; 2019: 1–16

[22] A. D. Damavandi, M. Masih-Tehrani, and B. Mashadi, “Configuration development and optimization of hydraulically interconnected suspension for handling

and ride enhancement,” *Proc. Inst. Mech. Eng. Part D J. Automob. Eng.*, vol. 236, no. 2–3, pp. 381–394, 2022.

[23] Gheibollahi, H., & Masih-Tehrani, M. (2023). A multi-objective optimization method based on NSGA-II algorithm and entropy weighted TOPSIS for fuzzy active seat suspension of articulated truck semi-trailer. *Proceedings of the Institution of Mechanical Engineers, Part C: Journal of Mechanical Engineering Science*, 09544062231151799.